A hadronic model for gamma-ray loud quasars

R.J. Protheroe,[1] A.-C. Donea[1,2]
(1) Department of Physics, University of Adelaide, Adelaide 5005, Australia
(2) Astronomical Institute of Romanian Academy, Bucharest, 75212, Romania

Abstract

We discuss the spectral energy distribution (SED) of quasars in a hadronic model having both internal and external target photon fields. The high energy part of the SED results from a cascade initiated by electrons from charged pion decay and Bethe-Heitler pair production and gamma-rays from neutral pion decay, and involves synchrotron radiation, inverse-Compton scattering and photon-photon pair production. We apply this model to 3C 273.

1. Introduction

Various hadronic models of active galactic nuclei (AGN) have been proposed [1]. Here, we consider a model in which a power-law distribution of protons is injected in an emission region in an AGN jet, and follow the hadronic and electromagnetic cascades in the radiation and magnetic environment of the emission region. The output from these cascades will be cosmic rays and neutrinos (if the pion photoproduction threshold is exceeded) and gamma-rays which form the high energy part of the AGN spectrum. We apply such a model to the SED of quasars, and use as an example 3C 273.

3C 273 is the brightest and nearest (z= 0.158) quasar and has a small scale jet that extends up to 50 kpc from the core [2]. Its broad-band spectrum consists of two spectral components which appear as 'humps' in the SED. The low-energy component comprises a 'big blue bump' (BBB) plus a continuum extending from the radio to UV or X-ray frequencies which is generally believed to be synchrotron emission from relativistic electrons in the jet. The origin of the high-energy component, starting at X-ray and extending to energies above 100 MeV [3], is uncertain. We model the BBB with an accretion disk in symbiosis with the jet (an ADJ [4]). A detailed analysis of the UV peak in [5] suggests that the disk makes an inclination angle with the line of sight of up to $\theta \sim 60^\circ$. The uncertainty in θ allows a large range of possible Doppler factors for 3C 273.

pp. 2675–2678

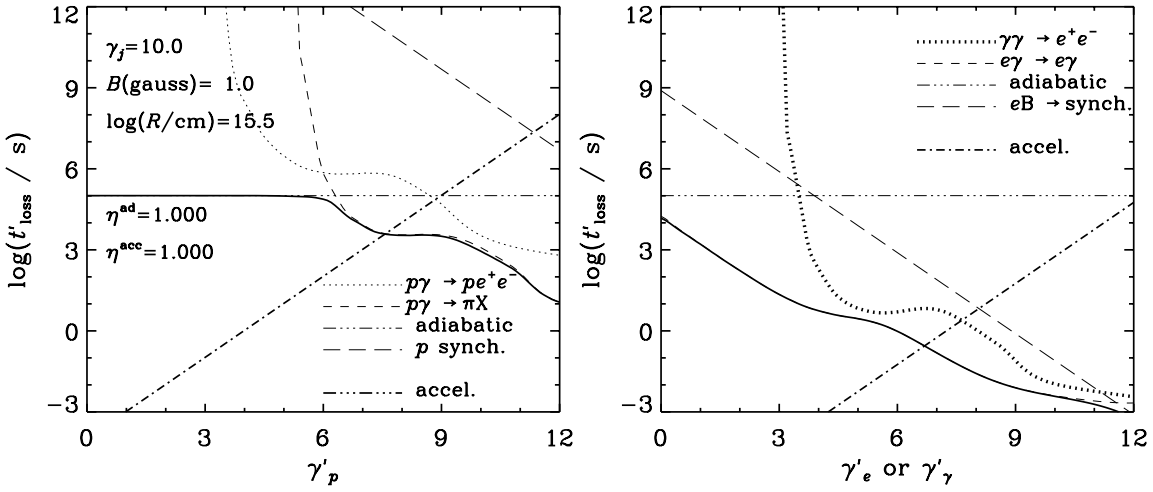

Fig. 1. Time scale for interaction, energy-loss, and acceleration for an emission region of radius 0.001 pc in the jet at distance 0.01 pc above the accretion disk of 2C273. (a) Protons. (b) Electrons of energy $\gamma'_e m_e c^2$ and photons of energy $\gamma'_\gamma m_e c^2$.

2. Hadronic and electromagnetic cascade

In the present example, we take the target radiation fields of 3C 273 to include the accretion disk, torus, and broad line region radiation, as seen inside an emission region at 0.01 pc moving at a jet Lorentz factor of 10. We also include the synchrotron component of directly accelerated electrons (which is assumed to comprise the non-disk component of the low-energy hump of the SED) as it would appear inside an emission region of radius 0.001 pc.

The jet-frame time-scales of protons, whose directions are assumed to be continuously randomised in a 1 Gauss magnetic field, are given in Fig. 1(a) which shows separately time-scales for Bethe-Heitler pair production and pion photoproduction, as well as adiabatic losses, synchrotron losses, and the shortest acceleration timescale possible given this magnetic field. In a numerical/Monte Carlo code we inject an $E_p'^{-2}$ power-law (dashed means jet-frame) extending to $E'_{p,\,\rm max} = 3 \times 10^6$ GeV, and allow it to cascade in the radiation/magnetic environment of the expanding emission region until all protons are below threshold for Bethe-Heitler pair production (treated as described by [6], photoproduction is treated using SOPHIA [7]).

The jet-frame time-scales of electrons (whose directions are assumed to be continuously randomised in a 1 Gauss magnetic field) and photons, are given in Fig. 1(b) which shows for photons: the pair production time (dotted), and for electrons: the synchrotron (long dashed), adiabatic (chain), inverse-Compton (short dashed) and total (solid). For electrons inverse-Compton scattering dominates.

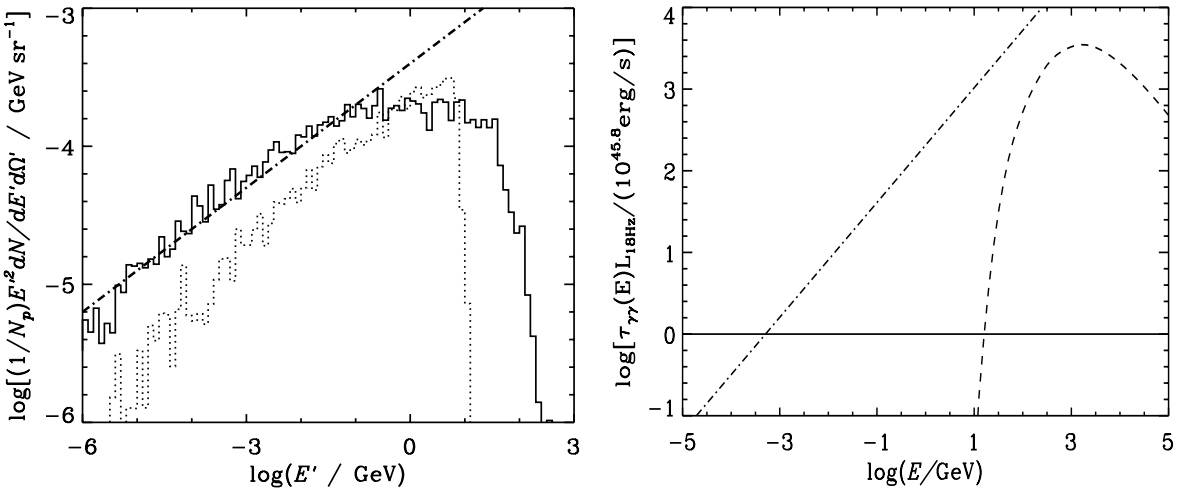

Fig. 2. (a) Jet-frame spectrum of photons at $\cos\theta' = -0.8$ (solid histogram) and $\cos\theta' = +0.8$ (dotted histogram) after hadronic and electromagnetic cascading. (b) Optical depth for model fit to 3C273 SED. Chain line shows optical depth internal to the emission region in an $E'^{-1.7}$ spectrum analogous to the cascade spectrum shown as the chain line in part a. Dashed curve gives the optical depth due to accretion disk radiation from the emission region to infinity along the jet axis.

The electrons and photons produced by the hadronic cascade are injected into the radiation/magnetic environment of the expanding emission region and their cascade followed until there are no photons remaining in the emission region – in the cascade photons above the pair production threshold have some probability of escaping. Electrons cool adiabatically, synchrotron radiate or inverse Compton scatter while being magnetically confined to the emission region. The spectrum of escaping gamma-rays is shown in Fig 2(a) for two jet-frame directions.

3. Fitting the SED of 3C 273

The observed high energy hump of 3C 273 and many quasars peaks near 1 MeV where the spectrum breaks from $\sim E^{-1.7}$ to $\sim E^{-2.5}$ and extends up to a few GeV. The cascade spectrum of escaping gamma-rays is shown in Fig 2(a) and has a slope which is reasonable for the region below the peak, but extends unbroken up to a few GeV. The (linear) cascading that resulted in Fig 2(a) included only external target photons and synchrotron target photons from directly accelerated electrons. However, the photon density of the cascade photons below 1 MeV provides significant pair-production optical depth to cascade photons above 1 MeV if the emission region radius is sufficiently small. The chain curve in Fig 2(b) shows the optical depth for the case of normalizing the chain curve

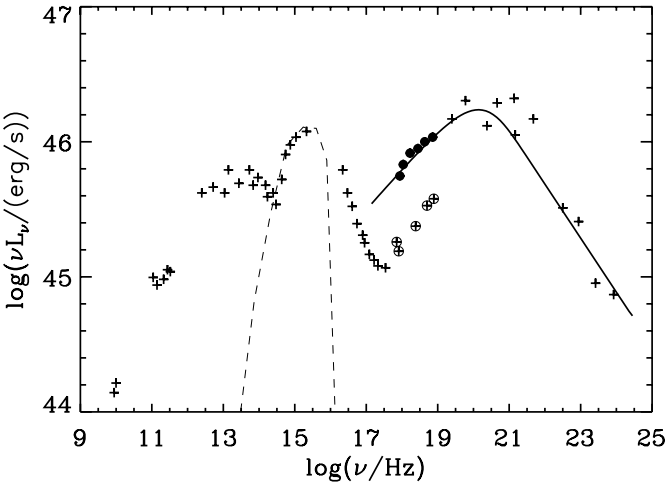

Fig. 3: SED of 3C273 showing assumed accretion disk component (dashed curve) and the best fitting high energy component (solid curve). The data points are taken from [2].

in Fig 2(a) to the observed SED at X-ray energies and using an emission region radius of 0.001 pc and a Doppler factor of 1.3. As can be seen, the optical depth is $\tau_{\gamma\gamma} = 1$ at ~ 0.5 MeV. In a rigorous calculation, one would treat the non-linear problem by solving the non-linear problem where the whole of the SED can provide target photons for the cascade. Instead, here we make the approximation that the spectrum after such a (non-linear) cascade can be obtained simply by multiplying the result from the linear cascade by $[1 - \exp(-\tau_{\gamma\gamma})]/\tau_{\gamma\gamma}$. Further absorption by external photons, e.g. from the accretion disk (dotted in Fig 2b) are negligible, as in this case is absorption outside the emission region by emission region photons. The resulting spectrum is plotted as the solid curve in Fig. 3.

Acknowledgments

This research if funded by the Australian Research Council.

References

1. Mannheim K., 1993, A&A 269, 67; Protheroe R.J., 1997, IAU Colloq. 163, ASP Conf. Series, Vol. 121, 585; Aharonian F., 2000, New Astronomy 5, 377; Mücke A., Protheroe R.J., 2001, Astropart. Phys. 15, 121; Atoyan A., Dermer C.D., 2001, Phys.Rev.Lett., 87, 221102
2. Kataoka J., Tanihata C., Kawai N, et al., 2002, MNRAS 336, 932
3. Collmar W., Reimer, O., et al., 2000, A&A 354, 513
4. Donea A.-C., Biermann P.L., 1996, A&A 316, 43
5. Kriss G., Davidsen A.F., Zheng W., Lee G, 1999, ApJ. 527, 683
6. Protheroe R.J., Johnson P.A., 1996, Astropart. Phys., 4, 253
7. Mücke A., et al., 2000, Comm.Phys.Comp., 124, 290